Hindawi Publishing Corporation
International Journal of Corrosion
Volume 2014, Article ID 256424, 11 pages
http://dx.doi.org/10.1155/2014/256424

Research Article

Corrosion Inhibition Effect of 4-Hydroxy-*N*′-[(*E*)-(1*H*-indole-2-ylmethylidene)] Benzohydrazide on Mild Steel in Hydrochloric Acid Solution

Preethi Kumari,[1] Prakash Shetty,[2] and Suma A. Rao[1]

[1]*Department of Chemistry, Manipal Institute of Technology, Manipal University, Manipal 576104, India*
[2]*Department of Printing and Media Engineering, Manipal Institute of Technology, Manipal University, Manipal 576104, India*

Correspondence should be addressed to Prakash Shetty; prakash.shetty@manipal.edu

Received 24 June 2014; Revised 13 November 2014; Accepted 13 November 2014; Published 11 December 2014

Academic Editor: Ramazan Solmaz

The inhibition performance and adsorption behaviour of 4-hydroxy-*N*′-[(*E*)-(1*H*-indole-2-ylmethylidene)] benzohydrazide (HIBH) on mild steel in 1 M HCl solution were tested by potentiodynamic polarization and electrochemical impedance spectroscopy (EIS). The inhibition efficiency of HIBH increases with increase in inhibitor concentration in the temperature range 30–60°C. Polarisation curves indicate that HIBH is a mixed inhibitor, affecting both cathodic and anodic corrosion currents. The adsorption process of HIBH at the mild steel/hydrochloric acid solution interface obeyed Langmuir adsorption isotherm model and inhibition takes place by mixed adsorption, predominantly chemisorption. The activation and thermodynamic parameters for the corrosion inhibition process were calculated to elaborate the mechanism of corrosion inhibition.

1. Introduction

The corrosion of iron and mild steel is a fundamental academic and industrial concern that has received a considerable amount of attention. Mild steel is widely employed as a constructional material in many chemical and petrochemical industries due to its excellent mechanical properties and low cost [1]. Acid solutions are widely used in industry, for example, acid pickling, chemical cleaning and processing, ore production, and oil well acidification [2]. Corrosion problems arise as a result of the interaction between the aqueous acid solutions and mild steel, especially during the pickling process in which the alloy is brought in contact with highly concentrated acids. This process if not combated can lead to economic losses due to the corrosion of the alloy [3]. Therefore corrosion control is essential in combating the negative environmental and industrial impact of corrosion. The use of inhibitors is one the most effective methods for protection against corrosion, especially in acidic media. Many heterocyclic compounds containing hetero atoms like nitrogen, sulphur, and/or oxygen atoms have been proved to be effective inhibitors for the corrosion of metals and alloys in acid media [4]. These organic compounds can adsorb on the metal surface, block the active sites on the surface, and thereby reduce the corrosion rate.

Hydrazides derivatives have continued to be the subjects of extensive investigation in chemistry and biology owing to their broad spectrum of antitumor [5], antimalarial [6], and many other applications as well as corrosion inhibition of metals. Several acid hydrazide derivatives, aromatic hydrazide derivatives, and thiosemicarbazide derivatives have shown exceptional ability to inhibit corrosion of mild steel in acidic solutions [7–9]. A survey of the literature reveals that, despite the high ability of hydrazide compounds to interact strongly with the metal surface, little attention has been paid to the use of these compounds as corrosion inhibitors. The inhibition property of these compounds is attributed to their molecular structure. The lone pair of electrons on the heteroatoms, the presence of π electrons, imine groups, electron donating groups, and the planarity of the entire structure are the important features that determine the adsorption of these molecules on the metallic surface.

The main objective of this work is to investigate the corrosion inhibition behaviour of 4-hydroxy-N'-[(*E*)-1*H*-indole-2-ylmethylidene)] benzohydrazide (HIBH) on mild steel in 1 M hydrochloric acid medium using potentiodynamic polarization and EIS techniques. The activation parameters for the dissolution process and thermodynamic parameters for the adsorption process are calculated. Further confirmation of the inhibition action of the compound is obtained by scanning electron microscopic analysis of the mild steel specimen in presence and absence of the inhibitor.

2. Experimental

2.1. Material. The material employed in the present work is mild steel with chemical composition of (% wt) C (0.159), Si (0.157), Mn (0.496), P (0.060), S (0.062), Cr (0.047), Ni (0.06), Mo (0.029), Al (0.0043), Cu (0.116), and balance iron. The specimen was prepared in the form of a cylindrical rod embedded in epoxy resin, having one end of the rod with an open surface area of 0.95 cm^2. The exposed flat surface of the mounted part was abraded using different grades of emery papers and finally on disc polisher using levigated alumina abrasive. The abraded specimen was washed with double distilled water, cleaned with acetone, and finally dried before immersing in the medium.

2.2. Medium. The acid solution (1.0 M HCl) is prepared by dilution of an analytical reagent grade 37% HCl with double-distilled water.

2.3. Inhibitor Preparation. 4-Hydroxy-N'-[(*E*)-1*H*-indole-2-ylmethylidene)] benzohydrazide (HIBH) is prepared as per the reported literature [6]. An equimolar mixture of ethanolic solution of indole-2-carboxaldehyde (0.01 mol) and 4-hydroxyl benzohydrazide (0.01 mol) is refluxed on a hot water bath for about 2 h. The precipitated product is filtered, dried, and recrystallized from ethanol. FTIR spectra of the recrystallized sample are recorded using spectrophotometer (Schimadzu FTIR 8400S) in the frequency range of 4000 to 400 cm^{-1} using KBr pellets. The chemical structure of the HIBH molecule is given in Figure 1.

2.4. Electrochemical Measurement. Electrochemical measurements are carried out using a potentiostat (CH Instrument USA Model 604D). Both polarization studies and electrochemical impedance measurements (EIS) are carried out using conventional three-electrode Pyrex glass cell with platinum as counter electrode, saturated calomel electrode (SCE) as reference electrode, and mild steel as working electrode. Finely abraded mild steel specimen with 0.95 cm^2 surface area is exposed to acid solution without and with different concentrations of inhibitors and allowed to establish a steady-state open circuit potential (OCP). The potentiodynamic current versus potential curves is recorded by polarizing the specimen from −250 mV cathodically to +250 mV anodically with respect to OCP with a scan rate of 1 mVs^{-1}. The experiments are performed at different temperatures using a calibrated thermostat. Corrosion potential (E_{corr}) and corrosion current density (i_{corr}) are recorded, from which corrosion rate (CR) and percentage inhibition efficiency (% IE) are obtained. EIS measurements are carried out in a frequency range from 0.01 to 10000 Hz using a small amplitude ac signal of 10 mV at the open circuit potential. Impedance data are analyzed using Nyquist plots. Charge transfer resistance (R_{ct}) and double layer capacitance (C_{dl}) are recorded.

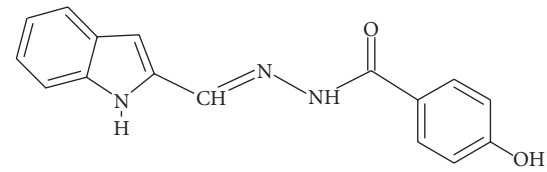

Figure 1: Chemical structure of HIBH molecule.

2.5. Scanning Electron Microscopy (SEM). The surface morphologies of the mild steel specimen immersed in 1 M hydrochloric acid solution in the presence and absence of optimal concentration of HIBH are compared by recording the SEM images of the specimen using a scanning electron microscope (EVO 18-5-57 model).

3. Results and Discussion

3.1. Characterization of HIBH. Crystalline yellow solid (95%); m. p: 154–158°C., IR (KBr) [cm^{-1}]: 1608 (C=N str.), 1770 (C=O), 1542 (Ar. C=C str.), 3035 (CH str.), 3182 (NH str.), 2719 (C–H assy. str.), 2796 (C–H sym. str.), 3610 (OH).

3.2. Potentiodynamic Polarization Studies. The effect of HIBH on the corrosion rate of mild steel was studied using Tafel polarization technique. Figure 2 shows the Tafel polarization curves for the dissolution of mild steel in 1 M hydrochloric acid solution at 40°C in the absence and presence of HIBH.

The corrosion rate (CR), the degree of surface coverage (θ), and the percentage inhibition efficiency (% IE) are calculated by using the following relations:

$$\mathrm{CR} = \frac{3270 \times M \times i_{corr}}{\rho \times Z}, \tag{1}$$

where 3270 is a constant that defines the unit of corrosion rate, i_{corr} is the corrosion current density in A cm^{-2}, ρ is the density of the corroding material, M is the atomic mass of the metal, and Z is the number of electrons transferred per metal atom [10]. Consider

$$\theta = \frac{i_{corr} - i_{corr(inh)}}{i_{corr}}, \tag{2}$$

where θ is the surface coverage and i_{corr} and $i_{corr(inh)}$ are the corrosion current densities in the absence and presence of HIBH, respectively [8]. Consider

$$\%\ \mathrm{IE} = \theta \times 100. \tag{3}$$

Electrochemical corrosion kinetic parameters such as corrosion potential (E_{corr}), cathodic Tafel slope (b_c), anodic

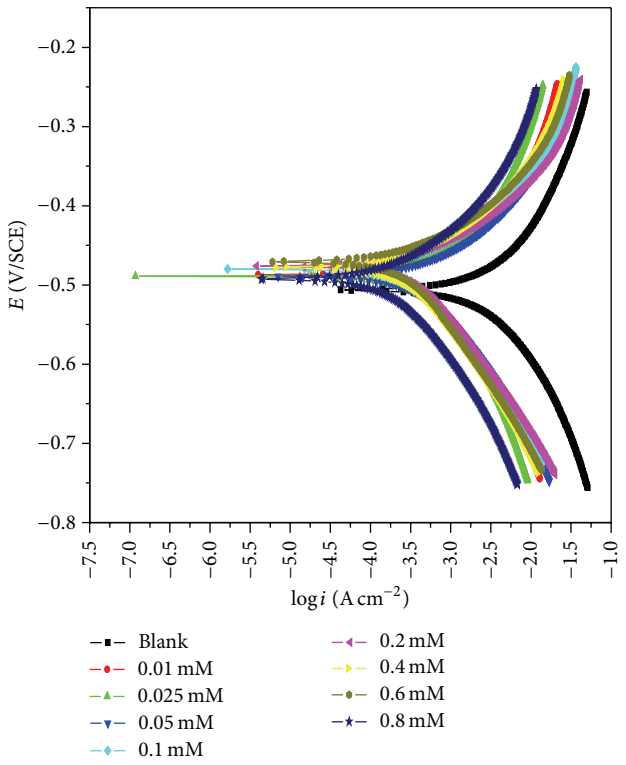

Figure 2: Tafel polarization curves for the mild steel specimen in 1 M HCl with various concentrations of HIBH at 40°C.

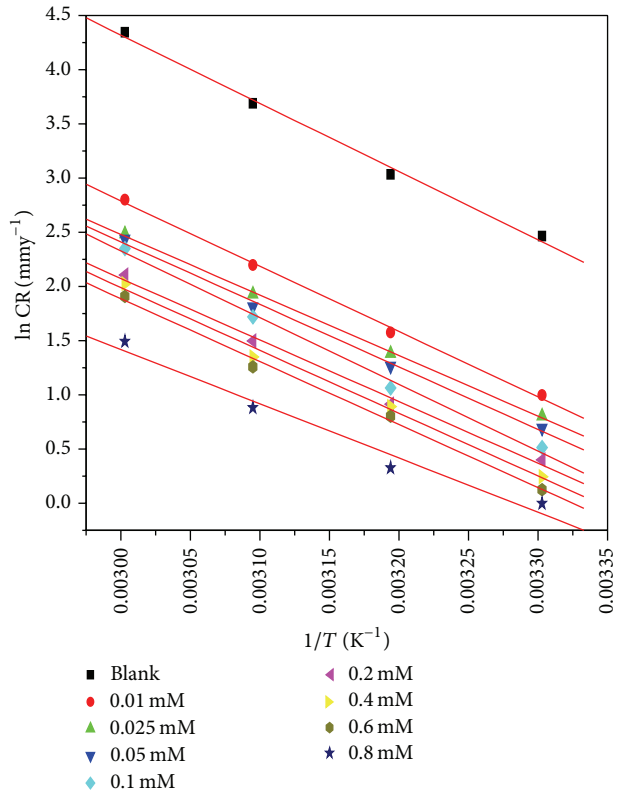

Figure 3: Arrhenius plots of ln(CR) versus $1/T$ for mild steel in 1 M HCl with different concentrations of HIBH.

Tafel slope (b_a), corrosion current density (i_{corr}), corrosion rate (CR), and the inhibition efficiency (% IE) are obtained and recorded in Table 1. As it is evident from the data presented in Table 1, i_{corr} values decrease sharply with increase in the concentration of HIBH. Also the % IE increases with increase in inhibitor concentrations of HIBH, which is presumably due to the blocking effect of the metal surface by both adsorption and film formation [11]. In addition to this % IE is also found to increase with the increase in temperature. The high inhibition efficiency of HIBH is mainly due to its strong bonding interaction with the metal surface. The strong bonding is generally attributed to higher electron densities at active functional groups, present in the adsorbate molecule [12]. It is clear from the Tafel plot that there is no much shift in the E_{corr} values in the presence of inhibitor compared to that in the absence of inhibitor. This indicates that HIBH acts as a mixed type of inhibitor by suppressing both anodic metal dissolution and cathodic hydrogen evolution reactions [11]. The slight variation in cathodic Tafel slopes (b_c) suggests the influence of HIBH on the kinetics of the hydrogen evolution reaction. This indicates an increase in the energy barrier for proton discharge, leading to less gas evolution [13]. Similarly the small change in the anodic slope (b_a) indicates that HIBH was first adsorbed onto the metal surface and impeded by merely blocking the reaction sites of the metal surface without affecting the anodic reaction mechanism [14].

The activation energy (E_a) for the corrosion and inhibition process was calculated [15] from Arrhenius plot according to the following equation:

$$\ln(\mathrm{CR}) = B - \frac{E_a}{RT}, \tag{4}$$

where B is the Arrhenius preexponential constant and R is the universal gas constant.

The plot of ln(CR) versus ($1/T$) gave a straight line (Figure 3) with slope equal to $-E_a/R$, from which the E_a values are calculated and tabulated in Table 2.

The enthalpy of activation ($\Delta H^{\#}$) and entropy of activation ($\Delta S^{\#}$) for the metal dissolution process are determined using the transition state equation [16]:

$$\mathrm{CR} = \frac{RT}{Nh} \exp\left(\frac{\Delta S^{\#}}{R}\right) \exp\left(\frac{-\Delta H^{\#}}{RT}\right), \tag{5}$$

where h is Plank's constant and N is Avogadro's number. The plot of ln(CR/T) versus $1/T$ gives a straight line (Figure 4) with slope equal to $-\Delta H^{\#}/T$ and intercept equal to $\ln(R/Nh) + \Delta S^{\#}/R$. From these results the $\Delta H^{\#}$ and $\Delta S^{\#}$ values are calculated and recorded in Table 2.

The energy of activation (E_a) obtained from the Table 2 is slightly lower than in the absence of inhibitor. This may be

Table 1: Tafel polarization results for the corrosion of mild steel in 1 M HCl in the absence and presence of inhibitor at different temperatures.

Temp. (°C)	Conc. of HIBH (mM)	E_{corr} (mV/SCE)	$-b_c$ (mV dec^{-1})	b_a (mV dec^{-1})	i_{corr} (mA cm^{-2})	CR (mmy^{-1})	% IE
30	0	−507	73.1	73.1	1.894	11.74	—
	0.01	−499	65.0	73.8	0.534	3.31	71.7
	0.025	499	69.2	99.8	0.486	3.01	74.3
	0.05	−498	68.9	112.3	0.374	2.45	80.2
	0.1	−481	73.5	119.3	0.269	1.67	85.7
	0.2	−481	78.2	113.4	0.240	1.49	87.3
	0.4	−482	76.6	102.4	0.206	1.28	89.1
	0.6	−488	73.2	102.7	0.183	1.13	90.3
	0.8	−502	78.8	115.7	0.161	1.00	91.4
40	0	−505	68.7	60.9	3.352	20.78	—
	0.01	−494	71.2	79.4	0.780	4.83	76.7
	0.025	−496	76.3	98.5	0.641	3.98	80.8
	0.05	−497	75.5	100.1	0.572	3.55	82.9
	0.1	−489	77.9	102.3	0.467	2.90	86.0
	0.2	−484	75.5	109.0	0.402	2.49	87.9
	0.4	−487	72.5	101.7	0.394	2.44	88.3
	0.6	−484	71.4	103.2	0.360	2.23	89.2
	0.8	−501	74.1	102.2	0.224	1.39	93.3
50	0	−504	61.3	57.8	6.458	40.03	—
	0.01	−501	55.9	78.2	1.417	8.80	78.0
	0.025	−499	72.6	82.5	1.104	6.88	82.9
	0.05	−499	70.5	95.4	0.994	6.14	84.6
	0.1	−495	64.9	95.4	0.900	5.58	86.1
	0.2	−491	71.8	98.1	0.720	4.47	88.8
	0.4	−497	77.3	97.0	0.622	3.85	90.3
	0.6	−495	78.0	105.8	0.567	3.52	91.2
	0.8	−499	77.5	105.0	0.389	2.41	93.9
60	0	−504	54.3	52.5	12.43	77.0	—
	0.01	−495	53.4	66.9	2.650	16.4	78.6
	0.025	−498	55.3	72.5	2.356	14.6	81.0
	0.05	−499	59.0	83.6	1.850	11.4	85.1
	0.1	−486	55.9	93.8	1.693	10.4	86.4
	0.2	−485	58.4	94.8	1.310	8.20	89.4
	0.4	−488	53.9	92.0	1.224	7.58	90.2
	0.6	−488	67.9	93.7	1.081	6.74	91.3
	0.8	−487	64.9	96.0	0.710	4.45	94.2

due to the slow rate of inhibitor adsorption with a resultant closer approach to the equilibrium at high temperature [17]. Riggs and Hurd [18] reported that the decrease in E_a in the presence of inhibitor may arise from a shift of the net corrosion reaction from the uncovered part of the metal surface to the covered one. Schmid and Huang [19] found that the organic molecules inhibit both anodic and cathodic partial reactions on the electrode surface and a parallel reaction takes place on the covered area, but the reaction rate on the covered area is substantially less than that on uncovered area which is similar to the present case.

Large negative values of $\Delta S^{\#}$ show that the activated complex in the rate determining step is an association rather than dissociation step meaning that a decrease in disordering takes place on going from reactants to the activated complex [20].

3.3. Electrochemical Impedance Spectroscopy. Electrochemical impedance spectroscopy (EIS) is a powerful analysis technique, which can be used to determine the characteristics and kinetics of electrochemical processes occurring at the metal/aggressive media interfaces. The corrosion behaviour of mild steel in 1 M HCl solutions in the absence and presence of different concentrations of HIBH is investigated by EIS at different temperatures and the impedance responses of the corrosion system are given in terms of Nyquist plot. As seen from Figure 5, the Nyquist plots consist of one depressed semicircle with a considerable deviation from an

Table 2: Activation parameters for the corrosion of mild steel in 1 M HCl acid containing different concentrations of HIBH.

Conc. of inhibitor (mM)	E_a (kJ mol^{-1})	$\Delta H^{\#}$ (kJ mol^{-1})	$-\Delta S^{\#}$ (J mol^{-1} K^{-1})
0	52.29	49.67	60.80
0.01	50.08	47.47	80.20
0.025	46.42	43.66	83.80
0.05	47.94	45.32	89.70
0.1	51.19	48.58	80.72
0.2	47.26	44.64	94.63
0.4	48.19	45.58	92.53
0.6	48.29	45.68	93.07
0.8	41.63	44.19	101.08

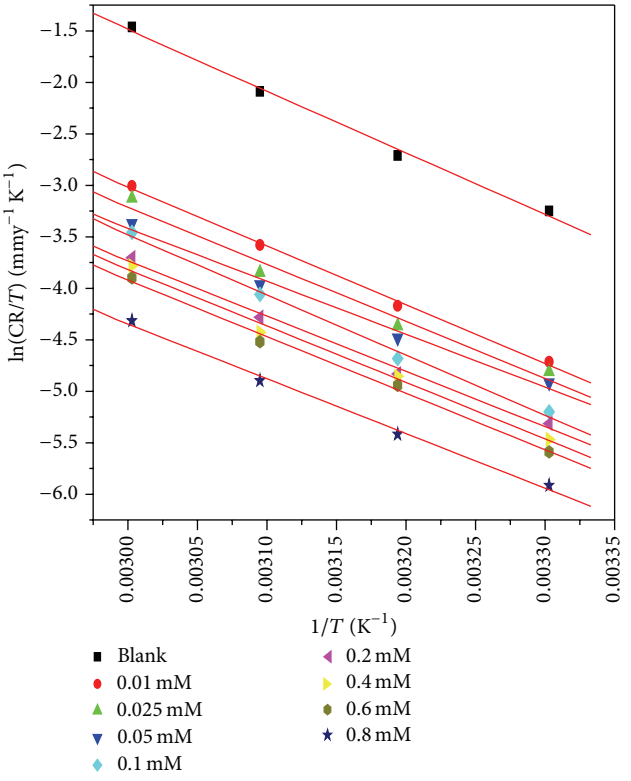

Figure 4: Plot of ln(CR/T) versus 1/T for mild steel specimen in 1 M HCl containing various concentrations of HIBH.

ideal semicircle and the diameter of semicircle increases with increasing inhibitor concentration. The existence of the same shape single semicircles shows the presence of single charge transfer process during dissolution which is unaffected by the presence of inhibitor molecules. The deviation from the perfect semicircle is generally attributed to the inhomogeneity and impurities of the metal electrode surface [19].

The impedance parameters are analysed by fitting a suitable equivalent circuit to the Nyquist plots using ZSimpWin software version 3.21. Figure 6 shows the simple Randles circuit, which is used to fit the impedance data in the absence

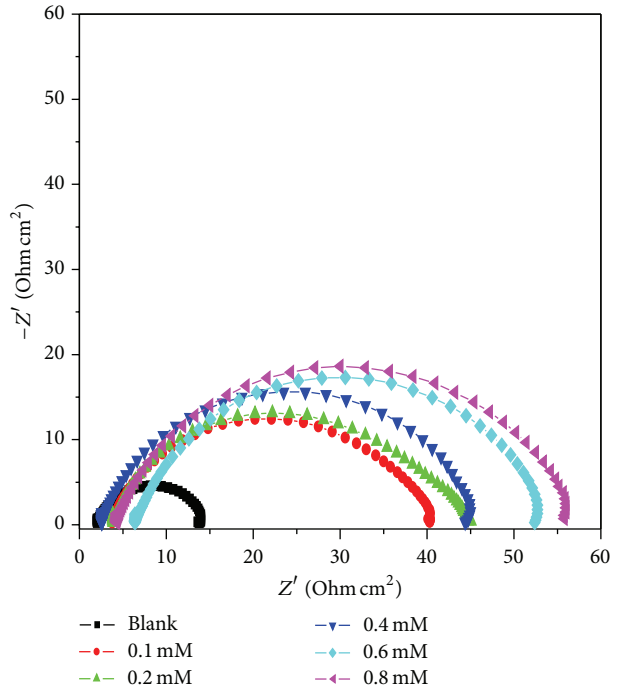

Figure 5: Nyquist plots for the mild steel specimen in 1 M HCl acid containing different concentrations of HIBH at 40°C.

and presence of inhibitor. In this equivalent circuit, R_s is the solution resistance, R_{ct} is the charge transfer resistance, and CPE is the constant phase element.

The constant phase element, CPE, is introduced in the circuit instead of a pure double layer capacitor to fit more accurately the behaviour of the electrical double layer. The CPE impedance (Z_{CPE}) is calculated [20] using the following equation:

$$Z_{CPE} = Q^{-1}\left(iw_{max}\right)^{-n}, \tag{6}$$

where Q is the proportionality coefficient, w_{max} is the angular frequency, i is the imaginary number, and n is the exponent related to the phase shift. The values of phase shift (n) lie between 0 and 1 ($0 \le n \le 1$). This is related to the deviation of CPE from the ideal capacitive behaviour. The correction in the capacitance to its real value (C_{dl}) is calculated [21] using the following equation:

$$C_{dl} = Q\left(w_{max}\right)^{n-1}. \tag{7}$$

The impedance parameters such as R_{ct} and C_{dl} are listed in Table 3. The values of % IE obtained from the charge transfer resistances are calculated using the following equation:

$$\%\ \text{IE} = \frac{R_{ct} - R_{ct}^{o}}{R_{ct}} \times 100, \tag{8}$$

where R_{ct} and R_{ct}^{o} indicate the charge transfer resistance in the presence and absence of HIBH, respectively.

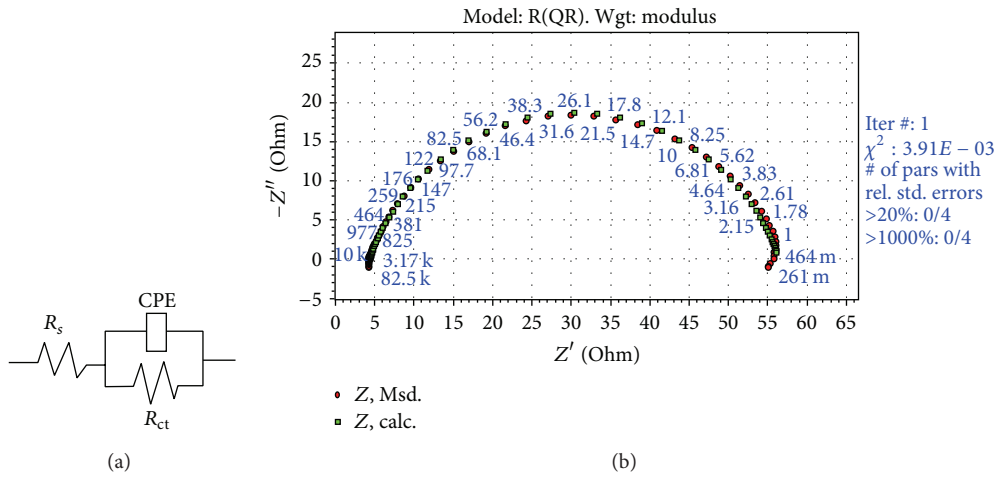

(a) (b)

Figure 6: Equivalent circuit used to fit the experimental EIS data (a). EIS data obtained for the corrosion inhibition of mild steel in 1 M HCl containing 0.8 mM HIBH at 40°C (b).

Table 3: Electrochemical impedance parameters for the corrosion of mild steel in 1 M HCl in the absence and presence of inhibitor at different temperatures.

Temp. (°C)	Conc. of HIBH (mM)	R_{ct} (Ω cm^2)	C_{dl} (μF cm^{-2})	n	% IE
30	0	15.70	1785	0.705	—
	0.1	89.55	84.31	0.732	82.5
	0.2	96.64	67.50	0.753	83.7
	0.4	101.5	64.19	0.757	84.5
	0.6	115.1	54.61	0.763	86.3
	0.8	122.0	50.58	0.766	87.1
40	0	9.63	3761	0.765	—
	0.1	60.07	207.4	0.767	83.9
	0.2	62.10	166.3	0.778	84.5
	0.4	66.39	141.2	0.795	85.4
	0.6	71.74	121.3	0.799	86.5
	0.8	76.35	94.24	0.817	87.3
50	0	5.00	12936	0.773	—
	0.1	31.99	540.4	0.768	84.3
	0.2	33.75	450.1	0.778	85.1
	0.4	36.35	401.1	0.788	86.2
	0.6	40.47	350.3	0.795	87.6
	0.8	42.5	289.8	0.82	88.2
60	0	1.90	55870	0.742	—
	0.1	13.41	2333.8	0.756	85.8
	0.2	13.81	2158.4	0.762	86.2
	0.4	14.86	1945.8	0.794	87.2
	0.6	15.90	1709.0	0.807	88.0
	0.8	18.55	1304.7	0.82	89.7

It is evident from Table 3, as the inhibitor concentration increases, the R_{ct} value is also found to increase. This can be explained based on covered effect, that is, the extent of adsorption of inhibitor on the metal surface. The surface coverage (θ) of an organic substance on the metal surface depends not only on the structure of the organic substance but also on the nature of the metal, experimental conditions, and concentration of molecules [22]. The surface coverage increases with the increase in inhibitor concentration. Since more inhibitors molecules are expected to adsorb at high inhibitor concentrations, the covered effect is enhanced. This results in an increase in R_{ct} and decrease in corrosion rate [23].

On the other hand, the capacitance of the interface (C_{dl}) starts decreasing, with increase in inhibitor concentration, which is most probably due to the decrease in local dielectric constant and/or increase in thickness of the electrical double layer. This suggests that the inhibitor acts via adsorption at the metal/solution interface [24]. Further the decrease in the C_{dl} values is also caused by the gradual replacement of water molecules by the adsorption of the inhibitor molecules on the electrode surface, which decreases the extent of metal dissolution [25].

3.4. Adsorption Isotherm. The primary step in the action of inhibitor in acid solution is generally due to the adsorption on the metal surface. This involves the assumption that the corrosion reactions are prevented from occurring over the area (or active sites) of the metal surface covered by adsorbed inhibitor species. The surface coverage (θ) is very useful for discussing the adsorption characteristics. The dependence of the surface coverage on the concentration of the inhibitor was tested graphically by fitting it to Langmuir's adsorption isotherm. Figure 7 shows the linear plots for C_{inh}/θ versus C_{inh}, suggesting that the adsorption obeys Langmuir's isotherm [26] given by the following equation:

$$\frac{C_{inh}}{\theta} = \frac{1}{K_{ads}} + C_{inh}, \tag{9}$$

where C_{inh} is the inhibitor concentration and K_{ads} is the adsorptive equilibrium constant, obtained from the reciprocal of

Table 4: Thermodynamic parameters for the adsorption of HIBH on mild steel surface in 1 M HCl acid at different temperatures.

Temp. (°C)	K_{ads} (M^{-1})	Slope	R^2	$-\Delta G^{\circ}_{ads}$ (kJ mol^{-1})	ΔH°_{ads} (kJ mol^{-1})	$-\Delta S^{\circ}_{ads}$ (J mol^{-1} K^{-1})
30	131248.7	1.090	0.999	39.80	1.77	137.0
40	124518.1	1.083	0.999	40.98		
50	135438.6	1.069	0.999	42.53		
60	136477.0	1.067	0.999	43.85		

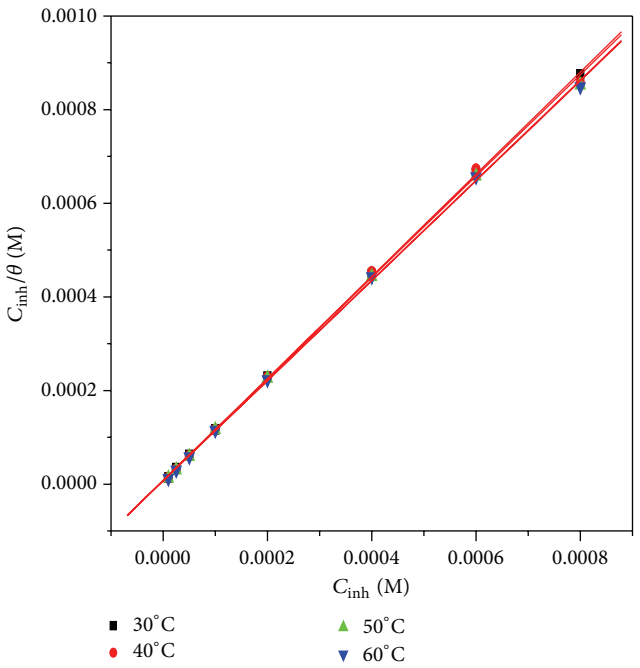

Figure 7: Langmuir's adsorption isotherm of HIBH on mild steel in 1 M HCl at different temperatures.

intercept of Langmuir plot lines. The slopes of the isotherms show deviation from the value of unity. This deviation from unity may be due to the interaction among the adsorbed species on the metal surface; that is, the organic molecules having polar atoms or groups get adsorbed on the cathodic and anodic sites of the metal surface by replacing the initially adsorbed water molecule [27].

The standard free energy of adsorption (ΔG°_{ads}) is related to K_{ads} by the following relation [28]:

$$K = \frac{1}{55.5} \exp\left(\frac{-\Delta G^{\circ}_{ads}}{RT}\right), \quad (10)$$

where R is the universal gas constant, T is the absolute temperature, and 55.5 is the concentration of water in solution in mol dm^{-3}. The calculated values of ΔG°_{ads} are tabulated in Table 4. Generally, the values of ΔG°_{ads} up to -20 kJ mol^{-1} are consistent with electrostatic interaction between the charged molecules and the charged metal (physisorption), while those around -40 kJ mol^{-1} or higher are associated with chemisorption as a result of sharing or transfer of electrons from the organic molecules to the metal surface to form a coordinate type of bond [29, 30]. In the present study the ΔG°_{ads} values obtained are close to 40 kJ mol^{-1} at 30 and 40°C and slightly more than 40 kJ mol^{-1} at 50 and 60°C, respectively. This indicates that the studied inhibitor may follow physical adsorption particularly at lower temperature and chemical adsorption at higher temperature.

The standard enthalpy of adsorption (ΔH°_{ads}) and the standard entropy of adsorption (ΔS°_{ads}) are computed from the slope and intercept of the straight line obtained by plotting ΔG°_{ads} versus T (Figure 8), according to the thermodynamic equation (11). The results are recorded in Table 4. Consider

$$\Delta G^{\circ}_{ads} = \Delta H^{\circ}_{ads} - T\Delta S^{\circ}_{ads}. \quad (11)$$

The positive values of enthalpy obtained (Table 4) indicate that adsorption of the inhibitor molecule is an endothermic process. Generally an exothermic adsorption process signifies either physical adsorption or chemical adsorption, while the endothermic process is attributable unequivocally to chemical adsorption [31]. In the present investigation, positive value of enthalpy of adsorption proves that adsorption of the inhibitor is by a chemical adsorption process. The chemical adsorption is also consistent with the increase in the efficiency of the inhibitor with increase in temperature. The ΔS°_{ads} value is large and negative, indicating that the decrease in disordering takes place on going from the reactant to the adsorbed species. This can be attributed to the fact that adsorption is always accompanied by decrease in entropy [32].

3.5. Inhibition Mechanism. The adsorption mechanism for a given inhibitor depends on factors, such as the nature of the metal, the corrosive medium, the pH, and the concentration of the inhibitor as well as the functional groups present in its molecule [33]. The mechanism of inhibition can be predicted from the knowledge of the interaction between the inhibitor molecules and the surface of the metal. In acid solution the mechanism of dissolution of mild steel [34] takes place as follows.

At anodic region,

$$Fe + Cl^{-} \longleftrightarrow (FeCl^{-})_{ads} \quad (12)$$

$$(FeCl^{-})_{ads} \longleftrightarrow (FeCl)_{ads} + e^{-} \quad (13)$$

$$(FeCl)_{ads} \longrightarrow (FeCl)^{+} + e^{-} \quad (14)$$

$$(FeCl)^{+} \longleftrightarrow Fe^{2+} + Cl^{-} \quad (15)$$

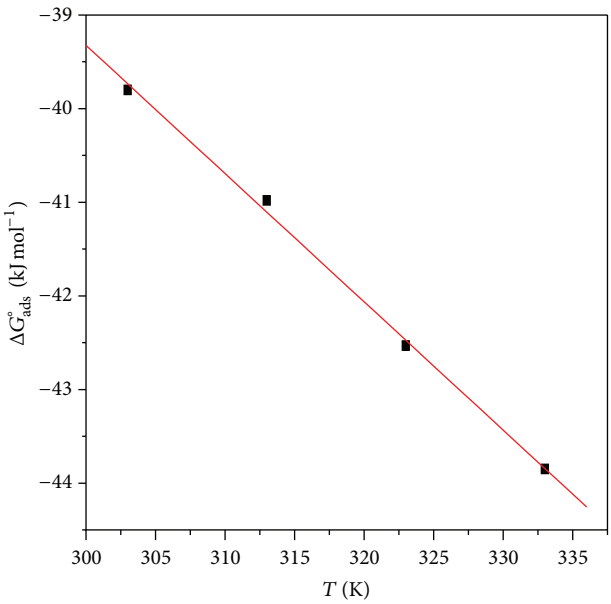

FIGURE 8: Plot of ΔG°_{ads} versus temperature for the adsorption of HIBH on mild steel in 1 M HCl.

The major cathodic reaction is evolution of hydrogen gas according to the following steps:

$$\mathrm{Fe} + \mathrm{H}^{+} \longleftrightarrow \left(\mathrm{FeH}^{+}\right)_{\mathrm{ads}} \quad (16)$$

$$\left(\mathrm{FeH}^{+}\right)_{\mathrm{ads}} + \mathrm{e}^{-} \longrightarrow \left(\mathrm{FeH}\right)_{\mathrm{ads}} \quad (17)$$

$$\left(\mathrm{FeH}\right)_{\mathrm{ads}} + \mathrm{H}^{+} + \mathrm{e}^{-} \longrightarrow \mathrm{Fe} + \mathrm{H}_2 \quad (18)$$

The adsorption of the inhibitor molecule is often a displacement reaction [35] involving removal of adsorbed water molecules from the metal surface as shown in the following:

$$\mathrm{Inh}_{(\mathrm{sol})} + n\mathrm{H}_2\mathrm{O}_{(\mathrm{ads})} \longleftrightarrow \mathrm{Inh}_{(\mathrm{ads})} + n\mathrm{H}_2\mathrm{O}_{(\mathrm{sol})} \quad (19)$$

The inhibition effect of HIBH in hydrochloric acid solution can be explained as follows and the mode of adsorption of HIBH on mild steel surface is predicted in Figure 9.

In acid medium hydrazide derivative gets protonated on the hydrazide group, which results in the formation of positively charged inhibitor species; thus adsorption of the inhibitor on the mild steel surface may occur through the following ways.

(i) In the presence of HCl medium initially, the metal surface behaves as positively charged species.

(ii) The chloride ions first adsorbed at the metal/solution interface at the corrosion potential through electrostatic attraction force due to the excess positive charge at this interface. This process changes the charge of the solution side of the interface from positive to negative.

(iii) This negative charge will attract the protonated inhibitor molecule facilitating physical adsorption of HIBH. Thus, protonated HIBH molecules are able to electrostatically adsorb on the electrode surface covered with primary adsorbed chloride ions leading to physisorption [36]. In addition the protonated inhibitor molecules can also be adsorbed at cathodic sites of metal in competition with hydrogen ions. The adsorption of protonated HIBH molecules reduces the rate of hydrogen evolution reaction along with metal oxidation resulting in physisorption:

$$\mathrm{Fe} + \mathrm{Cl}^{-} \longleftrightarrow \left(\mathrm{FeCl}^{-}\right)_{\mathrm{ads}} + \mathrm{HIBH}^{+} \longleftrightarrow \left(\mathrm{FeCl}^{-}\mathrm{HIBH}^{+}\right)_{\mathrm{ads}} \longleftrightarrow \left(\mathrm{Fe\,HIBH}^{+}\right)_{\mathrm{ads}} + \mathrm{Cl}^{-} \quad (20)$$

Further the unprotonated or neutral molecule of HIBH can also adsorb via chemisorption on the vacant sites on the metal surface by either of the following.

(i) Sharing of electrons between the hetero atoms of HIBH and iron surface.

(ii) π electron interactions between the aromatic ring of the HIBH and the metal surface.

(iii) Charge transfer from the HIBH molecules to the metal surface to form a coordinate type of a bond, because the vacant 3d orbitals of iron can bond with inhibitor due to interaction of electron rich π-electron clouds of aromatic rings as well as unshared electron pairs on nitrogen or oxygen atoms leading to predominantly chemisorption [37].

3.6. Scanning Electron Microscopy. The SEM images of mild steel surfaces were recorded after its immersion in 1 M hydrochloric acid for three hours in the absence and presence of HIBH. The inspection of Figure 10(a) reveals clear pits with a small size distribution over the entire surface of the metal surface. Figure 10(b) shows the SEM images of mild steel surface exposed to 1 M HCl with the addition of 0.8 mM HIBH for 3 hours. There are no pits and cracks observed in the micrograph. The smooth metal surface obtained was fully covered with the inhibitor molecules and a protective inhibitor film was observed.

3.7. A Comparison of the Earlier Reported Hydrazide Derivative Inhibitors with HIBH. A good number of hydrazide derivatives have been reported as corrosion inhibitor of mild steel in acidic media. The inhibition efficiency of most of the reported hydrazide derivatives decreased with increase in temperature [7–9, 38–42]. Some of the reported hydrazide derivatives showed moderate inhibition efficiency (less than 80%) at their optimum concentration and some showed good inhibition efficiency only at very high inhibitor concentration level [8, 41, 42]. Most of the reported hydrazide derivatives followed physisorption [7–9, 38–41]. The present inhibitor HIBH showed good inhibition efficiency of greater than 90% even at low optimal concentration (8×10^{-4} M). The % IE of HIBH increases with increase in temperature. The inhibition behaviour of HIBH follows mixed adsorption, predominantly with chemisorption.

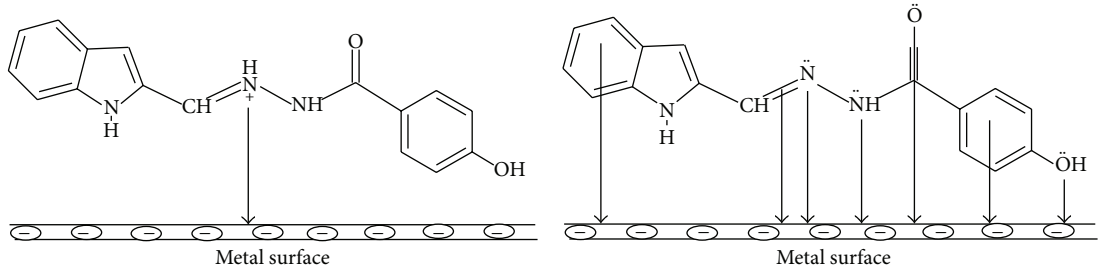

(a) (b)

Figure 9: Adsorption of HIBH on the mild steel surface through (a) electrostatic interaction and (b) electron pair interaction.

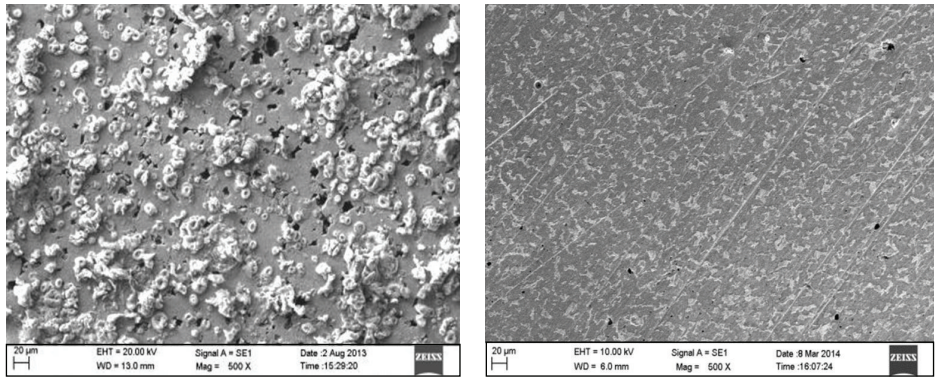

(a) (b)

Figure 10: SEM images of the mild steel specimen after immersion in 1.0 M HCl (a) in the absence and (b) in the presence of HIBH.

4. Conclusions

The conclusions drawn from the present study are as follows.

(1) HIBH is found to be a potential inhibitor for the corrosion control of mild steel in 1 M hydrochloric acid solution.

(2) Percentage inhibition efficiency increases with increase in HIBH concentrations and temperature.

(3) HIBH showed maximum inhibition efficiency, more than 90% at its optimum concentration at all the studied temperatures.

(4) HIBH acts as mixed type inhibitor.

(5) The adsorption of HIBH on the mild steel surface obeys Langmuir adsorption isotherm.

(6) The corrosion inhibition mechanism of HIBH follows mixed adsorption type with predominately chemisorption.

Conflict of Interests

The authors declare that there is no conflict of interests regarding the publication of this paper.

Acknowledgments

The authors are grateful to Manipal University and Manipal Institute of Technology, Manipal, for providing the laboratory facility.

References

[1] Z. Tao, S. Zhang, W. Li, and B. Hou, "Corrosion inhibition of mild steel in acidic solution by some oxo-triazole derivatives," *Corrosion Science*, vol. 51, no. 11, pp. 2588–2595, 2009.

[2] A. U. Ezeoke, N. O. Obi-Egbedi, C. B. Adeosun, and O. G. Adeyemi, "Synergistic effect of leaf extracts of *Cordia sebestena* L. and iodide ions on the corrosion inhibition of mild steel in sulphuric acid," *International Journal of Electrochemical Science*, vol. 7, no. 1, pp. 5339–5355, 2012.

[3] A. Y. El-Etre, "Inhibition of C-steel corrosion in acidic solution using the aqueous extract of zallouh root," *Materials Chemistry and Physics*, vol. 108, no. 2-3, pp. 278–282, 2008.

[4] A. El-Sayed, "Phenothiazine as inhibitor of the corrosion of cadmium in acidic solutions," *Journal of Applied Electrochemistry*, vol. 27, no. 2, pp. 193–200, 1997.

[5] S. Singh, F. Athar, and A. Azam, "Synthesis, spectral studies and in vitro assessment for antiamoebic activity of new cyclooctadiene ruthenium(II) complexes with 5-nitrothiophene-2- carboxaldehyde thiosemicarbazones," *Bioorganic and Medicinal Chemistry Letters*, vol. 15, no. 24, pp. 5424–5428, 2005.

[6] R. B. de Oliveira, E. M. de Souza-Fagundes, R. P. P. Soares, A. A. Andrade, A. U. Krettli, and C. L. Zani, "Synthesis and antimalarial activity of semicarbazone and thiosemicarbazone derivatives," *European Journal of Medicinal Chemistry*, vol. 43, no. 9, pp. 1983–1988, 2008.

[7] M. A. Quraishi, R. Sardar, and D. Jamal, "Corrosion inhibition of mild steel in hydrochloric acid by some aromatic hydrazides," *Materials Chemistry and Physics*, vol. 71, no. 3, pp. 309–313, 2001.

[8] A. V. Shanbhag, T. V. Venkatesha, R. A. Prabhu, R. G. Kalkhambkar, and G. M. Kulkarni, "Corrosion inhibition of mild steel in acidic medium using hydrazide derivatives," *Journal of Applied Electrochemistry*, vol. 38, no. 3, pp. 279–287, 2008.

[9] R. V. Saliyan and A. V. Adhikari, "Corrosion inhibition of mild steel in acid media by quinolinyl thiopropano hydrazone," *Indian Journal of Chemical Technology*, vol. 16, no. 2, pp. 162–174, 2009.

[10] U. M. Eduok, S. A. Umoren, and A. P. Udoh, "Synergistic inhibition effects between leaves and stem extracts of *Sida acuta* and iodide ion for mild steel corrosion in 1 M H_2SO_4 solutions," *Arabian Journal of Chemistry*, vol. 5, no. 3, pp. 325–337, 2012.

[11] M. Z. A. Rafiquee, N. Saxena, S. Khan, and M. A. Quraishi, "Some fatty acid oxadiazoles for corrosion inhibition of mild steel in HCl," *Indian Journal of Chemical Technology*, vol. 14, no. 6, pp. 576–583, 2007.

[12] M. Sangeetha, S. Rajendran, J. Sathiyabama et al., "Corrosion inhibition by an aqueous extract of *Phyllanthus amarus*," *Portugaliae Electrochimica Acta*, vol. 29, no. 6, pp. 429–444, 2011.

[13] S. T. Selvi, V. Raman, and N. Rajendran, "Corrosion inhibition of mild steel by benzotriazole derivatives in acidic medium," *Journal of Applied Electrochemistry*, vol. 33, no. 12, pp. 1175–1182, 2003.

[14] L. R. Chauhan and G. Gunasekaran, "Corrosion inhibition of mild steel by plant extract in dilute HCl medium," *Corrosion Science*, vol. 49, no. 3, pp. 1143–1161, 2007.

[15] M. Schorr and J. Yahalom, "The significance of the energy of activation for the dissolution reaction of metal in acids," *Corrosion Science*, vol. 12, no. 11, pp. 867–868, 1972.

[16] F. Bentiss, M. Lebrini, and M. Lagrenée, "Thermodynamic characterization of metal dissolution and inhibitor adsorption processes in mild steel/2,5-bis(n-thienyl)-1,3,4-thiadiazoles/hydrochloric acid system," *Corrosion Science*, vol. 47, no. 12, pp. 2915–2931, 2005.

[17] T. P. Hour and R. D. Holliday, "The inhibition by quinolines and thioureas of the acid dissolution of mild steel," *Journal of Applied Chemistry*, vol. 3, no. 11, pp. 502–513, 1953.

[18] L. O. Riggs Jr. and T. J. Hurd, "Temperature coefficient of corrosion inhibition," *Corrosion*, vol. 23, no. 8, pp. 252–260, 1967.

[19] G. M. Schmid and H. J. Huang, "Spectro-electrochemical studies of the inhibition effect of 4, 7-diphenyl -1, 10-phenanthroline on the corrosion of 304 stainless steel," *Corrosion Science*, vol. 20, no. 8-9, pp. 1041–1057, 1980.

[20] M. Mahdavian and M. M. Attar, "Electrochemical behaviour of some transition metal acetylacetonate complexes as corrosion inhibitors for mild steel," *Corrosion Science*, vol. 51, no. 2, pp. 409–414, 2009.

[21] I. Ahamad and M. A. Quraishi, "Mebendazole: new and efficient corrosion inhibitor for mild steel in acid medium," *Corrosion Science*, vol. 52, no. 2, pp. 651–656, 2010.

[22] S. John, B. Joseph, K. K. Aravindakshan, and A. Joseph, "Inhibition of mild steel corrosion in 1 M hydrochloric acid by 4-(N,N-dimethylaminobenzilidine)-3-mercapto-6-methyl-1,2,4-triazin(4H)-5-one (DAMMT)," *Materials Chemistry and Physics*, vol. 122, no. 2-3, pp. 374–379, 2010.

[23] A. Döner and G. Kardaş, "*N*-Aminorhodanine as an effective corrosion inhibitor for mild steel in 0.5 M H_2SO_4," *Corrosion Science*, vol. 53, no. 12, pp. 4223–4232, 2011.

[24] R. A. Prabhu, A. V. Shanbhag, and T. V. Venkatesha, "Influence of tramadol [2-[(dimethylamino)methyl]-1-(3-methoxyphenyl) cyclohexanol hydrate] on corrosion inhibition of mild steel in acidic media," *Journal of Applied Electrochemistry*, vol. 37, no. 4, pp. 491–497, 2007.

[25] M. Lagrenée, B. Mernari, M. Bouanis, M. Traisnel, and F. Bentiss, "Study of the mechanism and inhibiting efficiency of 3,5-bis(4-methylthiophenyl)-4H-1,2,4-triazole on mild steel corrosion in acidic media," *Corrosion Science*, vol. 44, no. 3, pp. 573–588, 2002.

[26] S. E. Frers, M. M. Stefenel, C. Mayer, and T. Chierchie, "AC-impedance measurements on aluminium in chloride containing solutions and below the pitting potential," *Journal of Applied Electrochemistry*, vol. 20, no. 6, pp. 996–999, 1990.

[27] S. Paul and B. Kar, "Mitigation of mild steel corrosion in acid by green inhibitors: yeast, pepper, garlic, and coffee," *ISRN Corrosion*, vol. 2012, Article ID 641386, 8 pages, 2012.

[28] O. Olivares, N. V. Likhanova, B. Gómez et al., "Electrochemical and XPS studies of decylamides of α-amino acids adsorption on carbon steel in acidic environment," *Applied Surface Science*, vol. 252, no. 8, pp. 2894–2909, 2006.

[29] I. Ahamad, R. Prasad, and M. A. Quraishi, "Thermodynamic, electrochemical and quantum chemical investigation of some Schiff bases as corrosion inhibitors for mild steel in hydrochloric acid solutions," *Corrosion Science*, vol. 52, no. 3, pp. 933–942, 2010.

[30] A. Yurt, G. Bereket, A. Kivrak, A. Balaban, and B. Erk, "Effect of Schiff bases containing pyridyl group as corrosion inhibitors for low carbon steel in 0.1 M HCl," *Journal of Applied Electrochemistry*, vol. 35, no. 10, pp. 1025–1032, 2005.

[31] M. A. Hegazy, H. M. Ahmed, and A. S. El-Tabei, "Investigation of the inhibitive effect of p-substituted 4-(N,N,N-dimethyldodecylammonium bromide)benzylidene-benzene-2-yl-amine on corrosion of carbon steel pipelines in acidic medium," *Corrosion Science*, vol. 53, no. 2, pp. 671–678, 2011.

[32] G. Banerjee and S. N. Malhotra, "Contribution to adsorption of aromatic amines on mild steel surface from HCl solutions by impedance, UV, and Raman spectroscopy," *Corrosion*, vol. 48, no. 1, pp. 10–15, 1992.

[33] S. Martinez and I. Stern, "Thermodynamic characterization of metal dissolution and inhibitor adsorption processes in the low carbon steel/mimosa tannin/sulfuric acid system," *Applied Surface Science*, vol. 199, no. 1–4, pp. 83–89, 2002.

[34] S. S. Abd El-Rehim, M. A. M. Ibrahim, and K. F. Khaled, "4-Aminoantipyrine as an inhibitor of mild steel corrosion in HCl solution," *Journal of Applied Electrochemistry*, vol. 29, no. 5, pp. 593–599, 1999.

[35] A. K. Singh and M. A. Quraishi, "Effect of Cefazolin on the corrosion of mild steel in HCl solution," *Corrosion Science*, vol. 52, no. 1, pp. 152–160, 2010.

[36] O. K. Abiola, A. O. C. Aliyu, A. A. Phillips, and A. O. Ogunsipe, "The effects of *Phyllanthus amarus* extract on corrosion and kinetics of corrosion process of aluminum in HCL solution," *Journal of Materials and Environmental Science*, vol. 4, no. 3, pp. 370–373, 2013.

[37] N. Hackerman, E. S. Snavely Jr., and J. S. Payne Jr., "Effects of anions on corrosion inhibition by organic compounds," *Journal of Electrochemical Society*, vol. 113, no. 7, pp. 677–686, 1966.

[38] V. R. Saliyan and A. V. Adhikari, "Quinolin-5-ylmethylene-3-[8-(trifluoromethyl)quinolin-4-yl]thiopropanohydrazide as an effective inhibitor of mild steel corrosion in HCl solution," *Corrosion Science*, vol. 50, no. 1, pp. 55–61, 2008.

[39] A. S. Fouda, M. T. Mohamed, and M. R. Soltan, "Role of some benzohydrazide derivatives as corrosion inhibitors for carbon steel in HCl solution," *Journal of Electrochemical Science and Technology*, vol. 4, no. 2, pp. 61–70, 2013.

[40] P. Mohan, K. A. Kumar, G. P. Kalaignan, and V. S. Muralidharan, "N′-(4-methoxybenzylidene) benzohydrazide as effective corrosion inhibitor for mild steel in 1 M HCl," *Asian Journal of Chemistry*, vol. 24, no. 12, pp. 5821–5823, 2012.

[41] L. Larabi, Y. Harek, O. Benali, and S. Ghalem, "Hydrazide derivatives as corrosion inhibitors for mild steel in 1 M HCl," *Progress in Organic Coatings*, vol. 54, no. 3, pp. 256–262, 2005.

[42] T. Gowrani, J. Yamuna, K. Parameswari, S. Chitra, A. Selvaraj, and A. Subramania, "The influence of benzoyl hydrazine and some of its substituents on corrosion inhibition of carbon steel in sulphuric acid solution," *Anti-Corrosion Methods and Materials*, vol. 51, no. 6, pp. 414–419, 2004.